CHAPTER VI

EXPERIMENTAL STUDY ON THE AZIMUTHAL ANCHORING OF A NEMATIC LIQUID CRYSTAL

6.1 Introduction

As we have already discussed in the previous chapter, the alignment of the nematic director on an appropriately treated substrate can be characterised by an anchoring energy. In that chapter we have described a new technique of estimating the anchoring energies for tilt orientation of the director at two plates of a I-IAN cell. In the present chapter we will study the influence of a transverse AC electric field on a nematic sample, which has a non-uniform alignment due to different pretilt angles at the two boundaries. The experiment enables us to estimate the azimuthal anchoring energy at these surfaces.

The splay and bend distortion in such a cell gives rise to a flexoelectric polarisation as discussed in earlier chapters. In Chapter IV we have described a technique of measuring the flexoelectric coefficient $(e_1 - e_3)$ by applying a transverse DC electric field on a hybrid aligned nematic cell. Here we use the electrooptic signal produced by a transeverse AC electric field to estimate the anchoring energies for azimuthal

orientation at the two surfaces of the cell. The applied AC electric field gives rise to a flexoelectric torque, which varies linearly with the field. This produces a twist distortion of tlie director without any threshold. Therefore ϕ oscillates at the frequency of the applied low frequency AC field. This in turn gives rise to an f component of the optical signal in the transmitted light. We have also developed a simple model for the electrooptic response of the system which allows us to estimate the azirnutlial anchoring energies at the two surfaces. There have been only a few earlier measurements of the azimuthal anchoring energy.

Three different experimental methods have been used earlier for the measurements of azimuthal anchoring energy (W_ϕ). Sicart *(1976)* used a twisted nematic cell in which one plate has stronger anchoring energy and the other is weakly anchored and measured change in twist angle as a function of an applied magnetic field. Faetti *et* al. *(1986, 1987)* used a torsion pendulum to measure the torque on the surface and hence calculated W_ϕ. Barbero *et al. (1986)* arid Toshi Oh-Ide *et al. (1988)* analysed tlie intensity of transmitted light to estimate the deviation of the director from the easy axis as a function of magnetic field and hence calculated W_ϕ. Later Faetti and Lazzari *(1992)* have used both reflection and transmission measurements to separate surface and bulk contributions and hence calculate W_ϕ. In a recent article Durand *(1993)* has reviewed some of the experiments on the anchoring properties of liquid crystals on amorphous solids.

6.2 Experimental Studies

6.2.1 Surface treatment

We have used three different types of surface treatments in our study.

1. In the first method, the glass plates were coated with silicon monoxide (SiO) vapour at an oblique angle of incidence ($\sim 35°$) with respect to its plane. This aligns the nematic director in the plane of the glass plate arid normal to the direction of incidence of SiO vapour. Further, there is no pretilt angle between the nematic director and the glass plate (Jannings, 1972).

2. In the second, the glass plates were coated with SiO vapour incident at a grazing angle of 5° with respect to the plane of the plate. In this case the direction of alignment is along the direction of incidence of SiO vapour and with a large tilt angle of 20" with respect to the plane of the substrate (Guyon *et* al., 1973). The SiO coating was sufficiently thick (>100 A.U.) to produce uniform alignment in the plane of incidence of SiO vapour (Monkade et al., 1988).

3. In the third technique the glass plates were coated with a polyimide solution and cured at 5G3 K. Then the plates were rubbed unidirectionally to get a homogeneous alignment of the nematic director in the plane of the glass plates. This produces a small pretilt angle of the order of 2° at the glass plates (Moslcy *et* al., 1987).

6.2.2 Cell preparation and pretilt angle measurement

Cells are prepared using glass plates appropriately treated to get the required pretilt angles. Two steel wires of diameter 20 μm and fixed on the plates with a separation of about 1000 μm between them are used as electrodes as well as spacers (Fig.6.1). The wires are arranged such that the electric field applied between them is orthogonal to the nematic director in the cell.

We have used a room temperature nematic liquid crystal, viz., *trans*-4-heptyl-(4-cyanophenyl)-cyclohexane (PCH-7) in our experiments.

For measuring the pretilt angle of the nematic director at the surface, we prepare

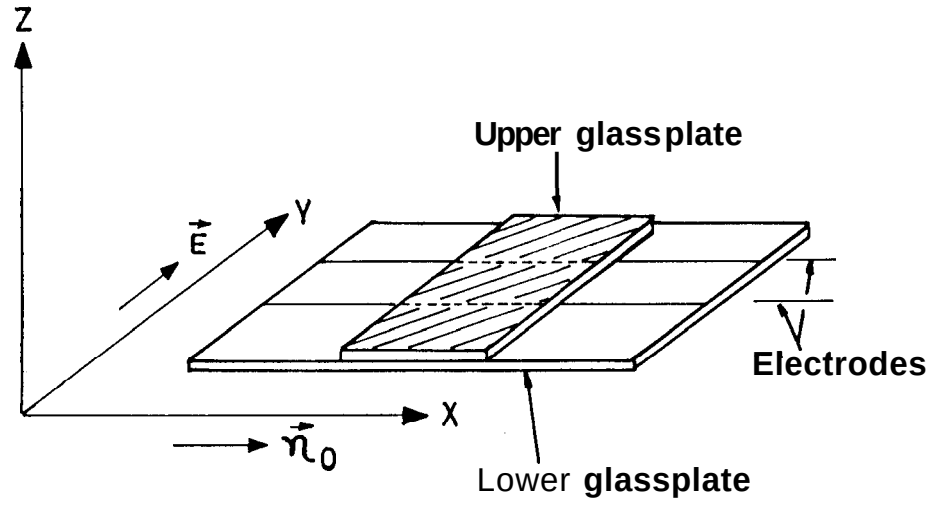

Fig.6.1 Cell geometry used in the experiment.

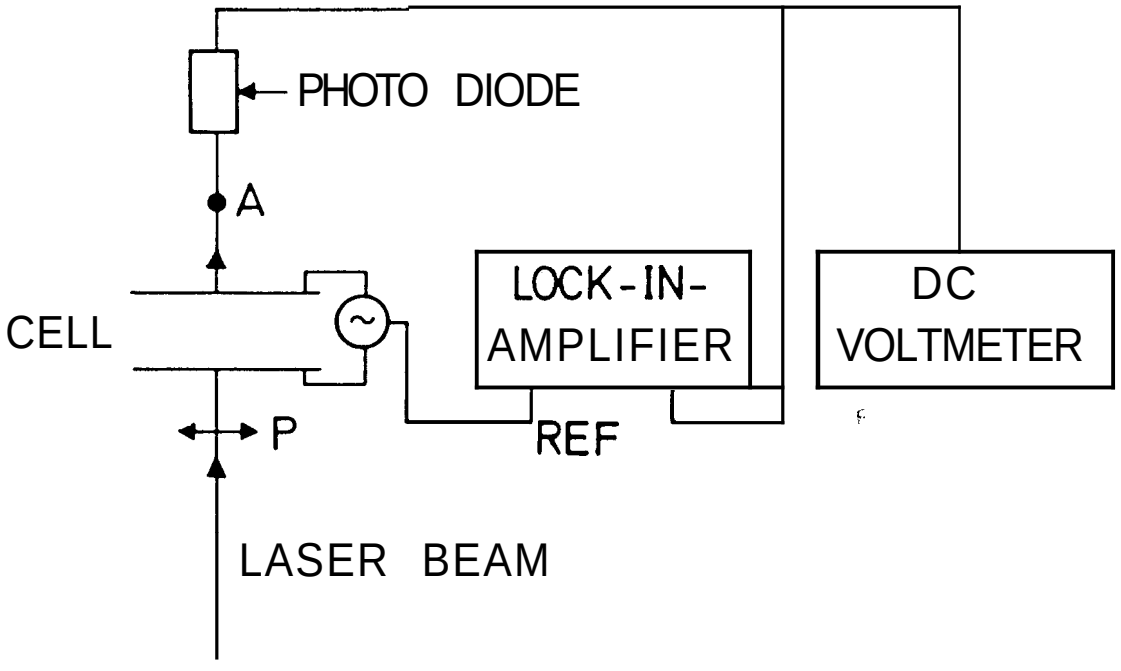

Fig.6.2 Block diagram of the experimental set up.

a cell with antiparallel orientation of the pretreated glass plates such that the sample has an uniform director field. Small pretilt angles ($\sim 2°$) have been measured using the technique described in Chapter II. For measuring large pretilt angles we used a different method. Let the nematic director make a pretilt angle 0 with the glass plate. Then the effective refractive index of the nematic liquid crystalline medium is given by

$$n_{eff}^2 = \frac{n_e^2 n_o^2}{n_o^2 \cos^2\theta + n_e^2 \sin^2\theta} \tag{6.1}$$

where n_e and n_o are the refractive indices for extraordinary and ordinary rays, or

$$\sin^2\theta = \frac{\frac{n_e^2 n_o^2}{n_{eff}^2} - n_o^2}{n_e^2 - n_o^2} \quad . \tag{6.1a}$$

Then the path difference introduced in the cell is

$$\Delta l = (n_{eff} - n_o)d \tag{6.1b}$$

where d is cell thickness. Using a tilting compensator (Leitz) the path difference **(Al)** is measured for a cell with uniform tilted director pattern. Using equation (6.1b), n_{eff} is calculated. Then using equation (6.1a), θ, the pretilt angle is calculated.

6.2.3 Electrooptic measurements

A block diagram of the experimental set up is shown in figure 6.2. The cell is placed in a Mettler hot stage (FP82) to regulate the temperature of the sample. The hot stage itself is mounted on the stage of a Leitz polarising microscope (Orthoplan) between crossed polarisers. A helium-neon laser (Uniphase) is used to illuminate the sample. AC field from the output of the lock-in-amplifier (PAR 5301A) is applied to the terminals of the cell. The transmitted light beam is monitored using a Centronics photo-diode (Model OSI 5K). The photodiode output is connected to DC nanovoltmeter (Keithley, Model 181) to measure the DC component of the signal and also connected to the lock-in-amplifier to measure the AC component of the

optical signal. We have measured the f , 2f and DC components of the intensity of the transmitted light. These signals are measured as functions of

(a) tlie applied AC field at a constant frequency,

(b) the frequency of the applied field at a constant voltage, and

(c) the azimuthal angle (ψ) made by the plane containing the director when E=O with respect to the polarizer. This is done by rotating the microscope stage through different angles, keeping the applied field and its frequency constant.

In order to facilitate comparison of these electrooptic signals with theoretical calculations, we have normalised the f and 2f signals with respect to their corresponding DC signals.

6.3 Results

6.3.1 Cells with *Planar* alignment without pretilt angle

The following observations correspond to a cell with SiO coating giving zero pretilt angle at both the surfaces (Fig.6.3a). Our measurements have been made at a temperature of 313 K.

1. In these cells the j signal was not observed at low voltages.
2. The 2f component of the signal is measurable only above a threshold voltage (V_{th}) and the f component of the signal appears at still higher fields (>45 V) (Fig.6.4).
3. The 2f signal is always greater than the f signal.
4. The 2f signal shows maxima at ψ =22.5° and 67.5' (Fig.6.5).

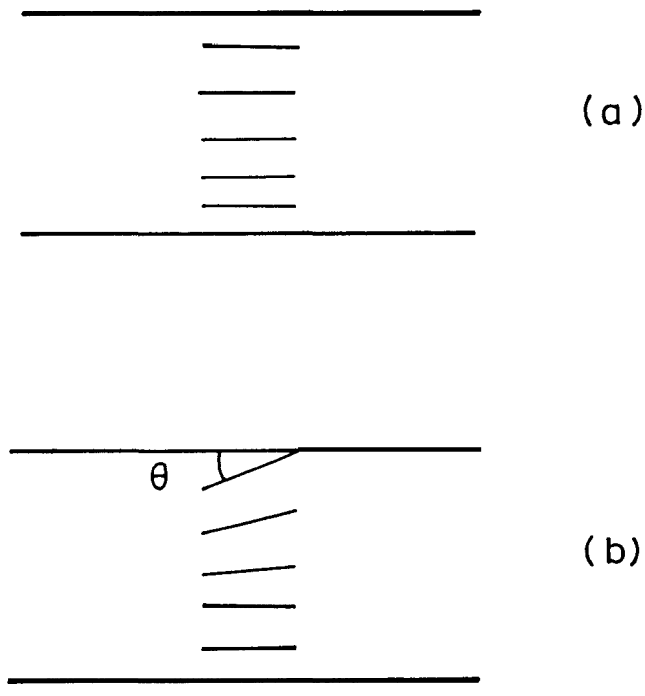

Fig.6.3 (a) Alignment of the director in a cell with a zero pretilt angle at the plates; (b) splay distortion of the director in a cell made of SiO coated plates to get pretilt angles of θ and 0 at the upper arid lower plates respectively.

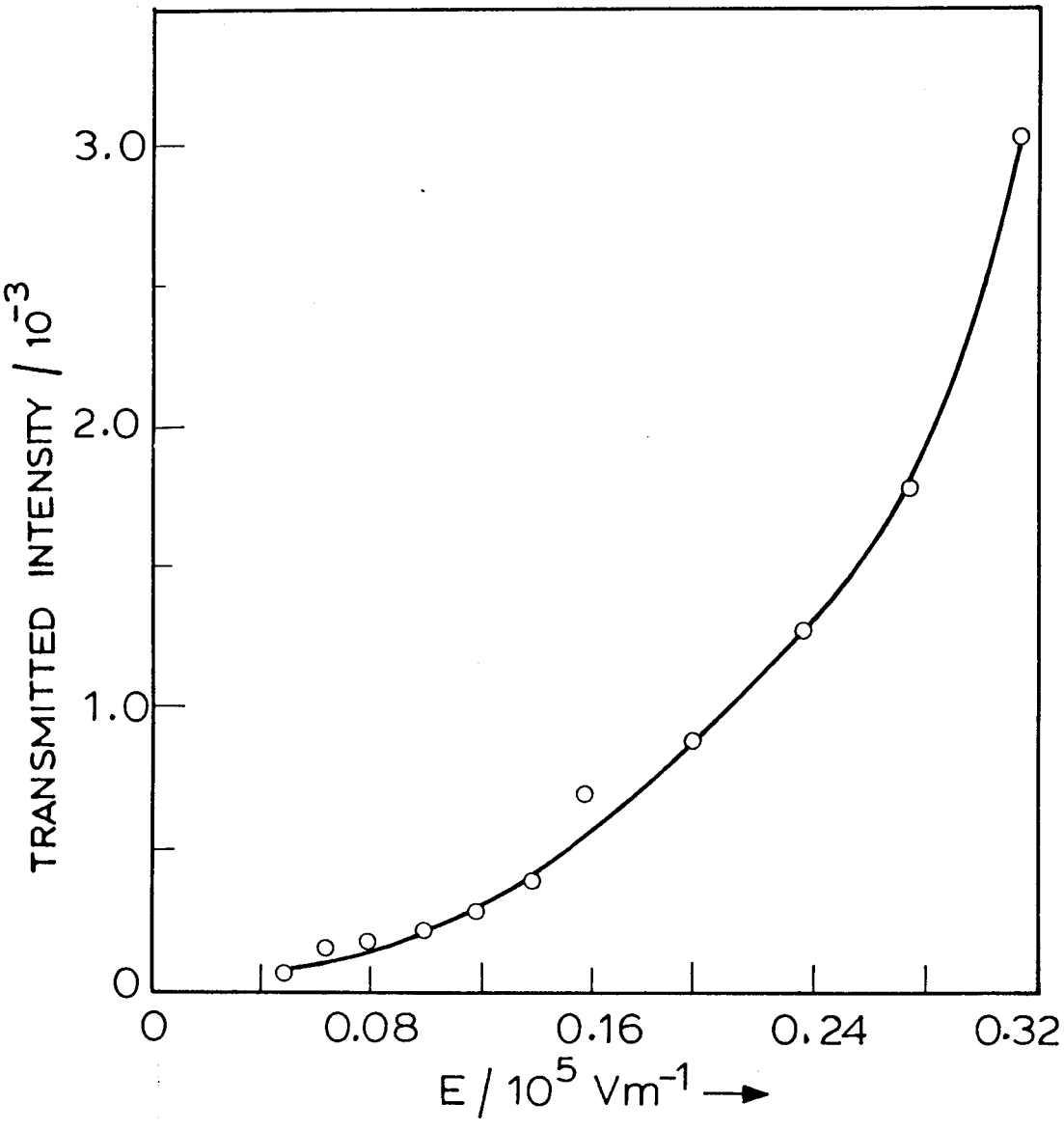

Fig.6.4 Field dependence of the $2f$ component of the transmitted intensity $\left(\frac{2f signal}{DC signal}\right)$ for a cell with its plates coated with SiO to get zero pretilt angle (θ=0). Cell thickness (D)=22.7 μm. Inter-electrode space (γ)=1275 μm, ψ=22.5°, frequency of the applied field (f)=7 Hz, Cell temperature (T)=313 K.

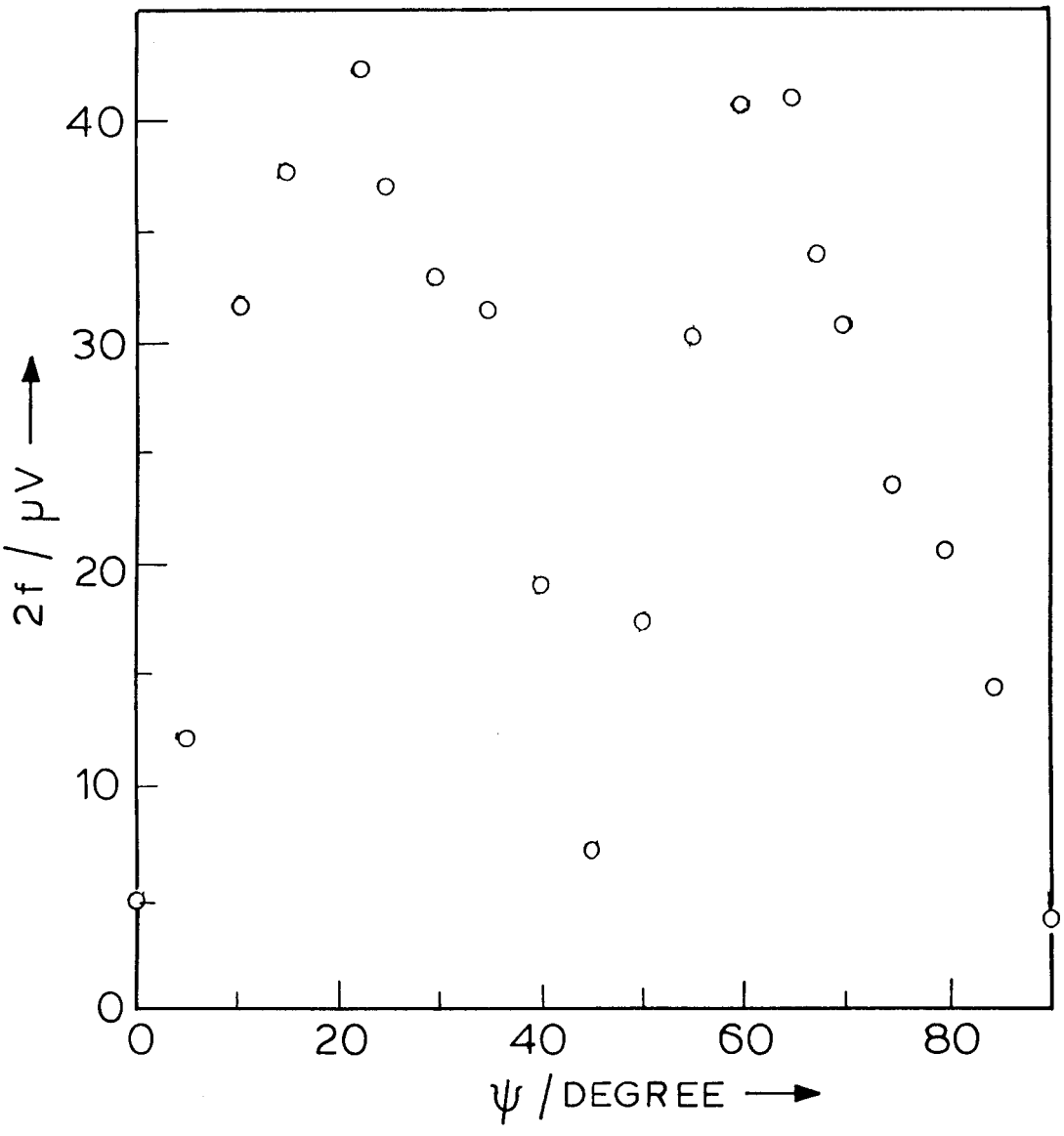

Fig.6.5 Variation of 2f signal with ψ for the cell described in Fig.6.4 at $E = 0.083 \times 10^5 V/m$, f=7Hz, T=313 K.

6.3.2 Cells with large splay distortion

These cells are made up of glass plates which are coated with SiO at appropriate angles of incidence. One of the plates has a large tilt angle ($\sim 20°$) and the other zero tilt angle of the director (Fig.6.3b). The following observations are made using such cells which have a large splay distortion of the director field.

1. An f signal is obscrvcd at arbitrarily low fields arid increases linearly with the applied field (Fig.6.6).

2. The 2f signal is measurable only when the field is sufficiently high and has a lower value than the f signal.

3. The f signal decreases steeply as the frequency of the applied field is increased (Fig.6.7).

4. The f signal shows maxima at azimuthal angles of 22.5" and 67.5° and a minimum at 45° as shown in figure 6.8.

6.3.3 Cells with small splay distortion

We have also prepared cells with one surface treated with polyimide and the other with SiO coating to get zero pretilt angle. In this cell the director profile will have a small pretilt angle ($\sim 2°$) at the polyimide surface. This type of cell also gives rise to an f signal at low fields which increases linearly with the applied field as in the previous case (Fig.6.9). However, the f signal is considerably reduced when compared to the f signal observed with large pretilt angles.

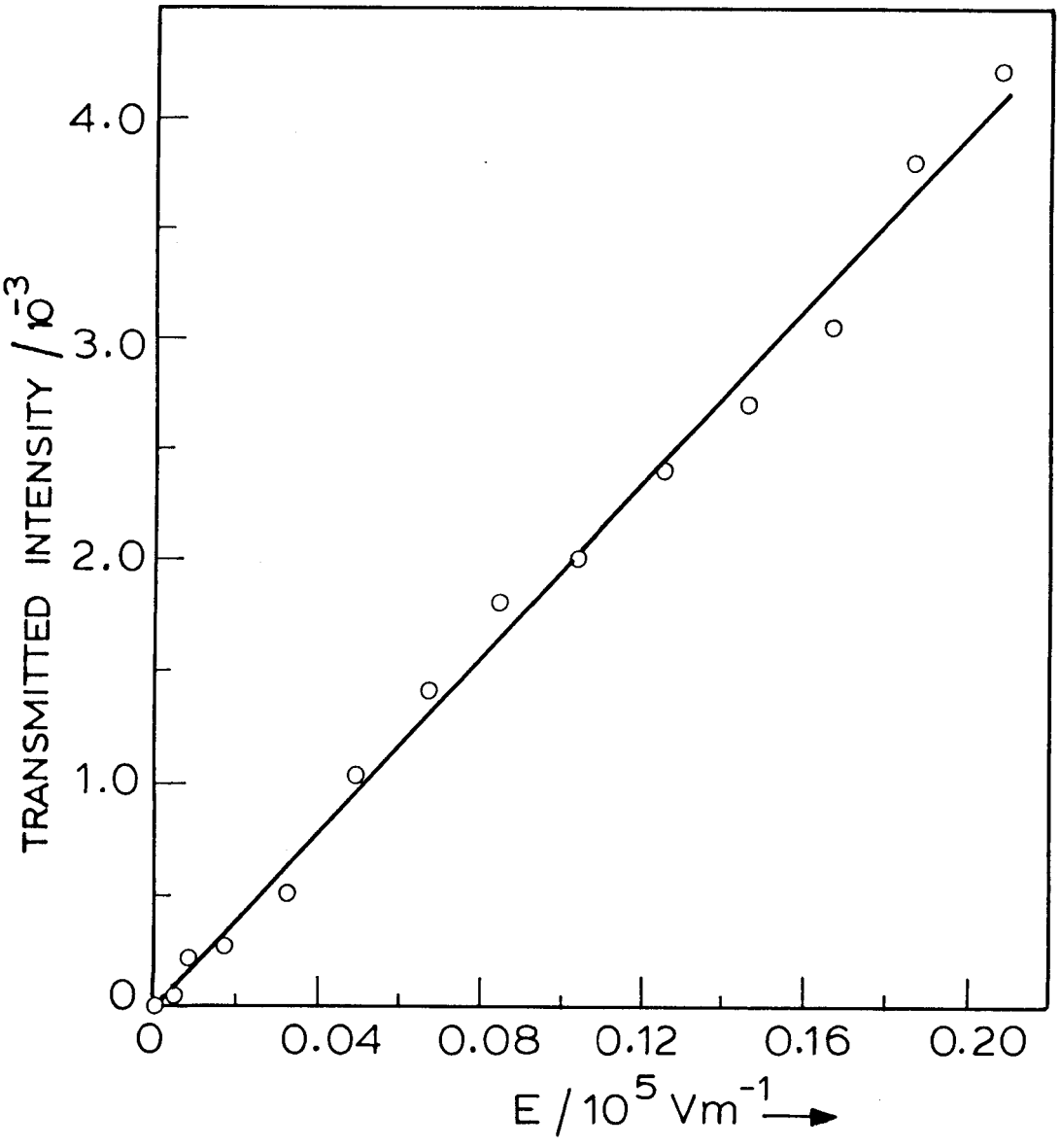

Fig.6.6 Field dependence of the f component of transmitted intensity $\left(\frac{f signal}{DC signal}\right)$ for a cell with a large splay distortion, $\theta_u \sim 20°$, $\psi = 22.5°$, $D = 24.2\ \mu m$, interelectrode space = 1200 μm, frequency = 7 Hz. Sample tremperature (T) = 313 K.

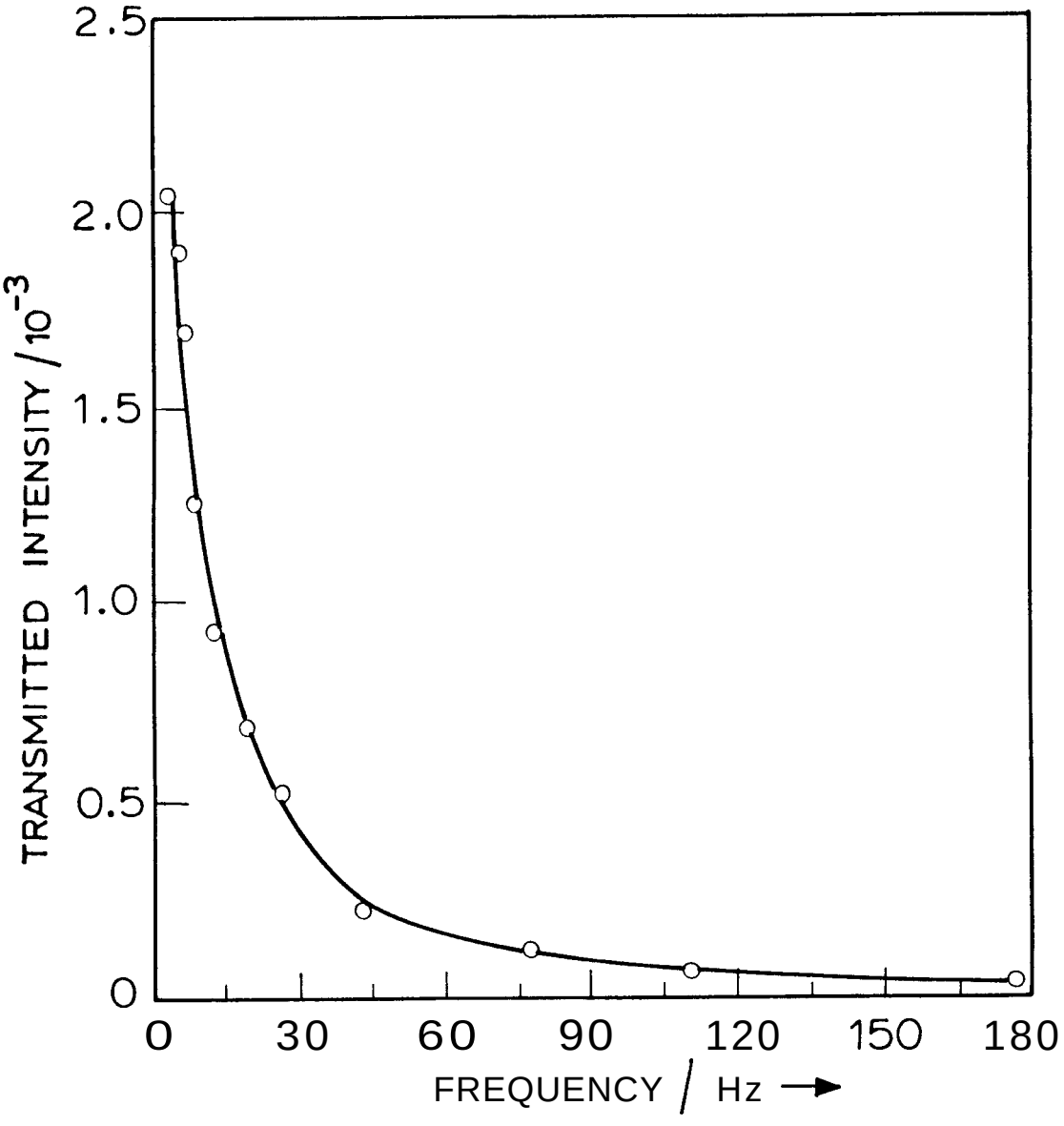

Fig.6.7 Frequency dependence of the f componerit of transmitted intensity $\left(\frac{I signal}{DC signal}\right)$ for the cell as in Fig.6.6 at $E = 0.083 \times 10^5 V/m$, T = 313 K.

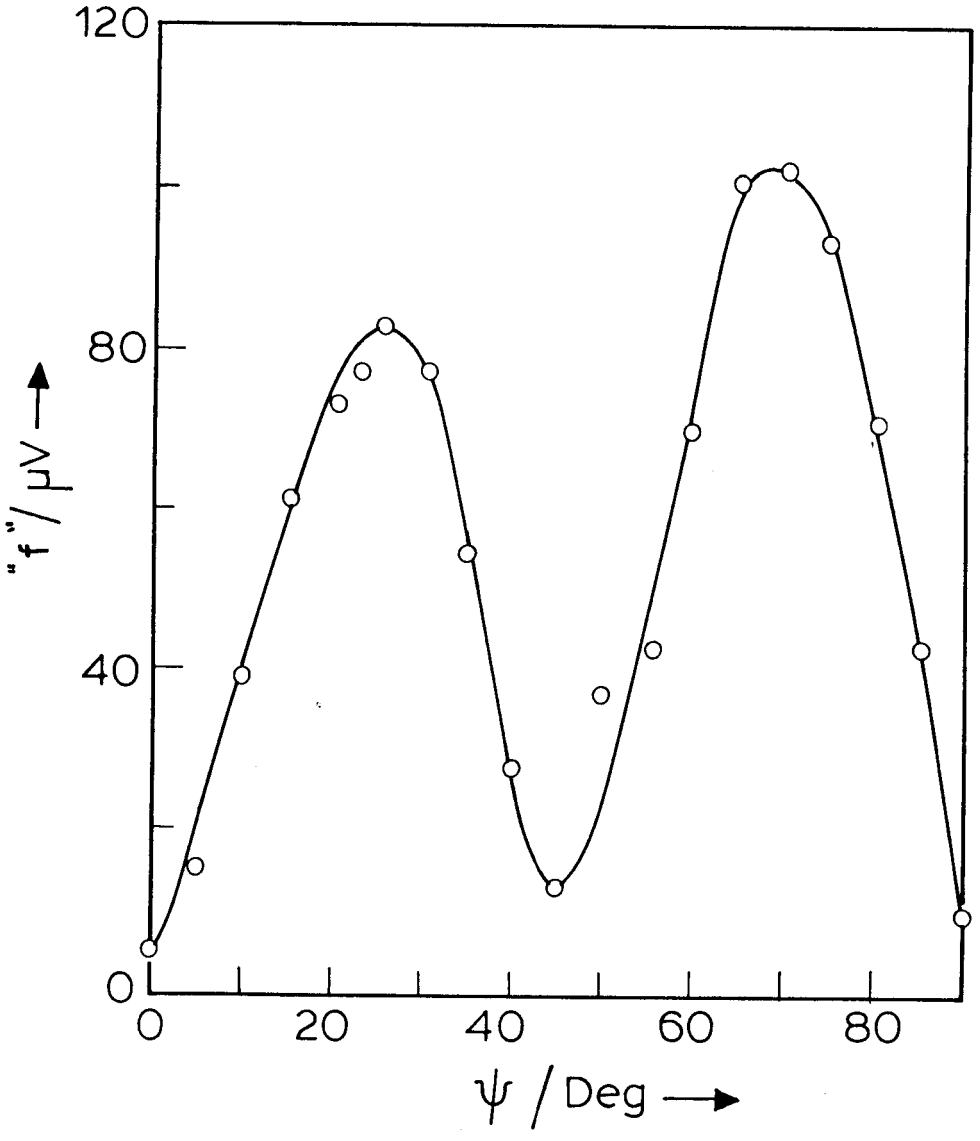

Fig.6.8 Azimuthal variation of "f" signal for the cell referred in fig. 6.6. $E = 0.083 \times 10^5 V/m$, $f = 7$ Hz, T = **313** K.

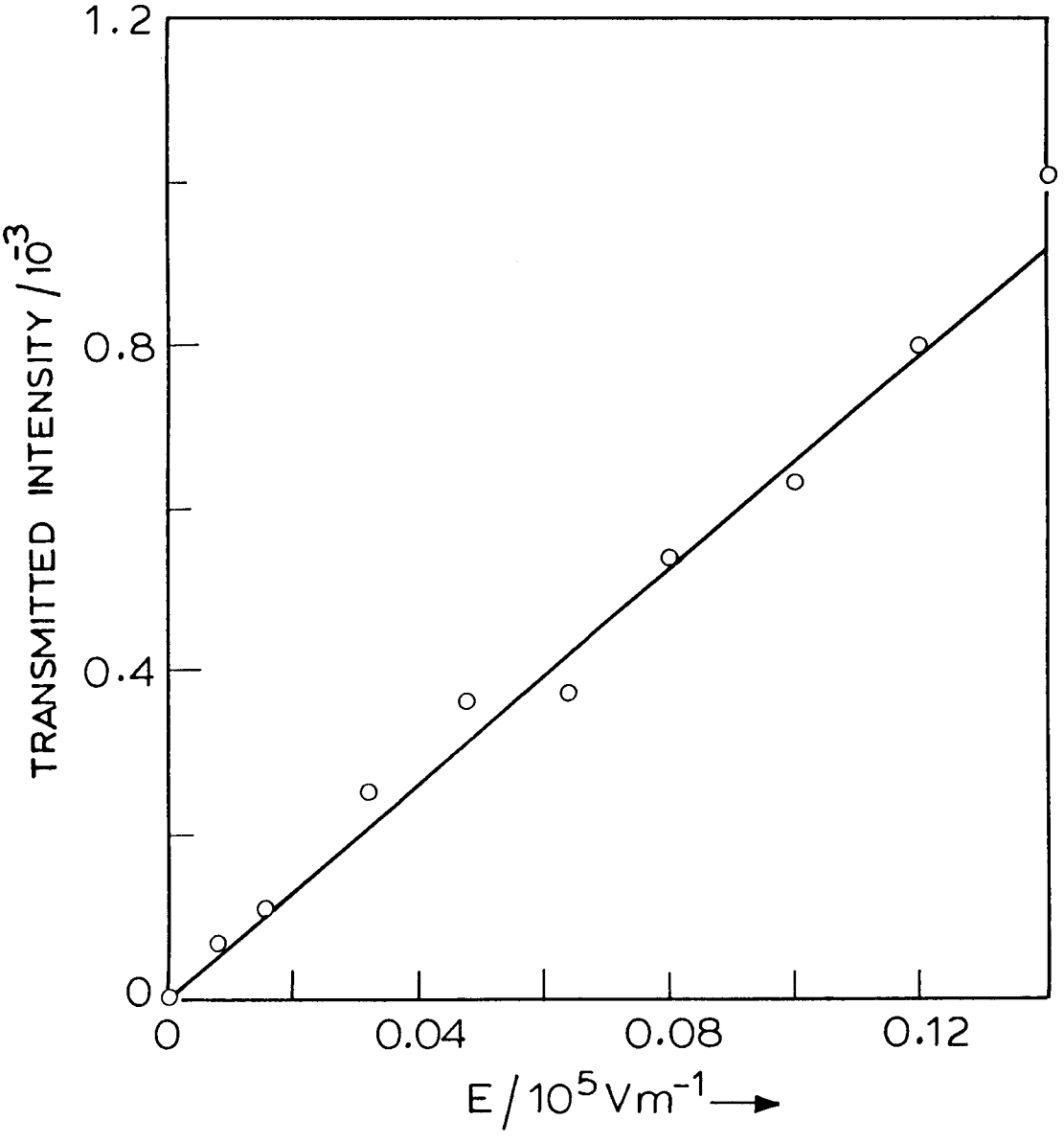

Fig.6.9 Field dependence of f component of transmitted intensity $\left(\frac{f signal}{DC signal}\right)$ for a cell with small splay distortion. $\theta \sim 2"$; $\psi = 22.5°$; $D = 22.8\ \mu m$; interelectrode space = 1250 μm. Frequency of the field f = 7 Hz. Sample temperature = 313 K.

6.4 Theoretical Analysis

The transmitted intensity of light beam propagating normal to the optic axis of a uniaxial medium between crossed polarisers is given by,

$$T_i = \frac{\sin^2 2\psi}{2}(1 - \cos \Delta\Phi) \ . \tag{6.2}$$

The application of the transverse AC electric field gives rise to azimuthal oscillations of the director. For a small variation of ψ we get

$$\mathrm{ST}(\$) = \sin 4\psi(1 - \cos \Delta\Phi)\Delta\psi \ .$$

ST has maxima at ψ = 22.5' and 67.5'. Hence the observation of such maxima in f and 2f signals implies corresponding ϕ oscillations of the director, where ϕ is the azimuthal angle of the director. On the other hand, θ oscillations of the director produce variations in the optical phase difference and in this case

$$\delta T(\theta) = \frac{\sin^2 2\psi}{2} \sin \Delta\Phi \, \delta(\Delta\Phi) \ .$$

Hence $\delta T(\theta)$ is a maximum at $\psi = 45°$.

We have analysed the AC electrooptical response of the cells with the splay deformation of $\hat{n}$ by using the following simplifications:

1. The one elastic constant approximation is used, i.e.,$K_1 = K_2 = K_3 = K$..
2. As we are interested in the f signal which varies linearly with the applied field (Fig.6.6), we have ignored dielectric torque which produces a quadratic effect with the applied field and hence the 2f signal.
3. From our measurements described in the previous chapter (V), W_θ, anchoring energy for tilt orientation is $\simeq 10^{-4} J/m^2$ For PCIJ-7 on a glass surface treated with polyimide solution. This corresponds to an extrapolation length, $K/W \simeq 10^{-8} m$, which is very much smaller than the typical cell thickness

$(20 \times 10^{-6} m)$. Hence we can assume even in this case that there is strong anchoring at the surface for tilt orientation. For SiO coated surface also the anchoring energy can be expected to be strong. Hence in our calculations we have assumed strong anchoring for θ distortion at both the surfaces of the cell.

4. We assume that the anchoring energies for the azimuthal orieritatiori arc W_l and W_u respectively at the lower and upper plates, i.e.,

$$F_{sl} = \frac{W_l}{2} \sin^2 \phi(O) \qquad \text{and} \qquad F_{su} = \frac{W_u}{2} \sin^2 \phi(D) \tag{6.3}$$

where D is thickness of the cell.

The geometry of the cell and the director $(\hat{n})$ profile are shown in figure 6.10. Under the action of the electric field E_y which acts along the Y axis, $\hat{n}$ develops a component n_y in the direction of the field, resulting in a twist deformation in the XY plane. Let θ_D be the tilt angle of the director at the upper plate. If 6 and ϕ are the tilt and azimuthal angles of the director, we have

$$n_x = \cos 6 \cos \phi, \quad n_y = \cos 6 \sin \phi, \quad \text{and} \quad \text{n,} = \sin \theta, \tag{6.4}$$

where θ and ϕ depend only on z.

We now calculate the various contributions to the energy density of the medium:

a) The elastic free energy density is given by,

$$F^{el} = \frac{K}{2} \left[\left(\frac{\partial n_x}{\partial z} \right)^2 + \left(\frac{\partial n_y}{\partial z} \right)^2 + \left(\frac{\partial n_z}{\partial z} \right)^2 \right] . \tag{6.5}$$

The components of elastic molecular field are

$$h_x^{el} = I\{ \frac{\mathrm{d}^2 \mathrm{n_x}}{\partial z^2}, \quad h_y^{el} = I\{ \frac{\mathrm{d}^2 \mathrm{n_y}}{\partial z^2}, \quad \text{and} \quad h_z^{el} = K \frac{\mathrm{d}^2 n_z}{\partial z^2} . \tag{6.6}$$

b) The flexoelectric energy density is given by,

$$F^{fl} = - \left(e_1 n_y \frac{\partial n_z}{\partial z} - e_3 n_z \frac{\partial n_y}{\partial z} \right) E_y . \tag{6.7}$$

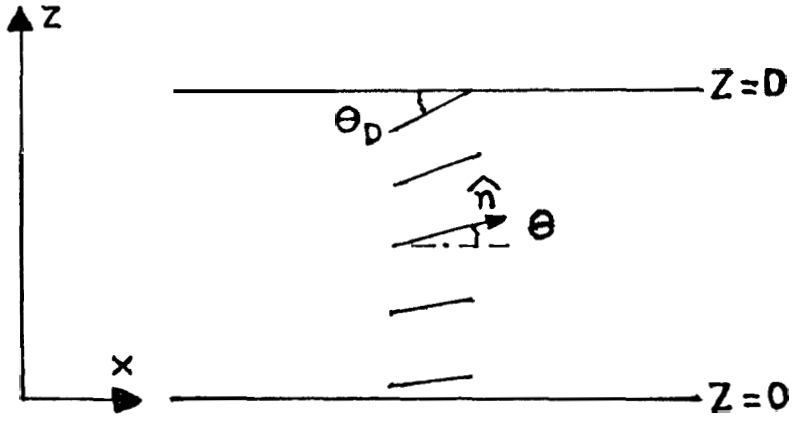

Fig.6.10 Figure showing the geometry of the cell and the director profile in a nematic cell with large splay distortion.

The components of flexoelectric molecular field are given by,

$$h_x = 0, h_y = E_y(e_1 - e_3)\frac{\partial n_z}{\partial z} \text{ and } h_z = -E_y(e_1 - e_3)\frac{\partial n_y}{\partial z} \quad . \tag{6.8}$$

c) Ignoring velocities, the components of **hydrodynamic molecular field** are given by (dc Gennes, 1975)

$$\begin{aligned} h_x^{hy} &= -\gamma_1 \sin 0 \cos\phi \frac{\partial\theta}{at}, \\ h_y^{hy} &= \gamma_1 \left(\cos\theta \cos\phi \frac{\partial\phi}{at} - \sin\theta \sin \$\frac{\partial\theta}{at}\right) \\ h_z^{hy} &= \gamma_1 \cos\theta \frac{\partial\theta}{at} \quad . \end{aligned} \tag{6.9}$$

The two independent components of the torque for an arbitrarily oriented director making tilt and azimuthal angles (θ and $\$$), have been worked out by Bodenschatz *et* al. (1988). They are given by,

$$\begin{aligned} \Gamma_2 &= \sin\theta(h_x \cos\phi + h, \sin\phi) - h, \cos\theta \\ &\simeq \sin\theta(h_x + \$11,) \quad - 11, \cos\theta \quad \text{for small}\,\phi \end{aligned} \tag{6.10}$$

$$\begin{aligned} \text{and } \Gamma_3 &= -h_x \sin\phi + h, \cos\phi \\ &\simeq -h_x\phi + h, \quad \text{for small}\,\phi \quad . \end{aligned} \tag{6.11}$$

Using these equations we get the local torque balance equations as,

$$-K\frac{\partial^2\theta}{\partial z^2} + E_y(e_1 - e_3)\cos^2\theta\frac{\partial\phi}{\partial z} = -\gamma_1\frac{\partial\theta}{\partial t} \tag{6.12}$$

and

$$K\left[\cos 8\frac{\partial^2\phi}{\partial z^2} - 2\sin\theta\frac{\partial\theta}{\partial z}\frac{\partial\phi}{\partial z}\right] + (e_1 - e_3)E_y \cos 0\frac{\partial\theta}{\partial z} = \gamma_1\cos\theta\frac{\partial\phi}{\partial t} \tag{6.13}$$

where we have ignored the dielectric term as we are interested only in the f-component of the signal.

The AC electric field applied to the cell is of the form

$$E_y = E_{yo} \sin wt \tag{G.14}$$

where $w = 2\pi f$, f is the frequency of the applied field.

Our experiments showed maxima of both f and 2f signals at ψ=22.5° and 67.5" which indicate oscillations of ϕ with the external field. Hence we assume that θ is time independent. The time independent part of equation (6.12) is then given by

$$\frac{\partial^2 \theta}{\partial z^2} = 0$$

or

$$\theta = C_1 Z + C_2, \tag{6.15}$$

where C_1 and C_2 are constants of integration.

The boundary conditions are: at $Z = 0$, θ=0 (at the lower plate) and hence C_2=0. At $Z = D$, i.e., at the upper plate, $\theta = \theta_D$, and we get

$$\theta = \frac{\theta_D}{D} Z \tag{6.16}$$

$$\frac{\partial \theta}{\partial z} = \frac{\theta_D}{D} . \tag{6.17}$$

As we will analyse only the f component we write the time dependent part of ϕ as

$$\phi_t = \phi_1 \sin 2\pi f t + \phi_2 \cos 2\pi f t \tag{6.18}$$

wliere ϕ_1 and ϕ_2 are the in-phase arid out of phase amplitudes, which are Z dependent.

Substituting for $\partial\theta/\partial z$ (equation 6.17) in equation (6.13), we get the in phase cornponent (i.e., the part depending on $\sin 2\pi f$t)

$$\frac{\partial^2 \phi_1}{\partial z^2} - \frac{2\theta_D}{D} tan\left(\frac{\theta_D}{D} z\right) \frac{\partial \phi_1}{\partial z} + \frac{E y_o (e_1 - e_3)}{K} \frac{\theta_D}{D} + \frac{\gamma_1 \omega}{K} \phi_2 = 0 .$$

A numerical estimate of the term $2\frac{\theta_D}{D} tan\left(\frac{\theta_D}{D} z\right) \frac{\partial \phi_1}{\partial z}$, by assuming $\theta_D \sim 0.3$ radians, shows that it is smaller by an order of magnitude when compared to the other terms in the above equation. Hence we ignore this term and simplify the above equation to get

$$\frac{\partial^2 \phi_1}{\partial z^2} + \frac{E_{yo}(e_1 - e_3)}{K} \frac{\theta_D}{D} + \frac{\gamma_1 \omega}{K} \phi_2 = 0 \ . \tag{6.19}$$

Similarly the out of phase component of equation (6.13) can be written as

$$\frac{\partial^2 \phi_2}{\partial z^2} - \frac{\gamma_1 \omega}{K} \phi_1 = 0$$

$$\text{or} \quad \phi_1 = \frac{K}{\gamma_1 \omega} \frac{\partial^2 \phi_2}{\partial z^2} \ . \tag{6.20}$$

Using equation (6.20) in equation (6.19) we get

$$\frac{\partial^4 \phi_2}{\partial z^4} + A^2 \phi_2 + C = 0 \tag{6.21}$$

where

$$A = \frac{\omega \gamma_1}{K} \quad \text{and} \quad C = \frac{(e_1 - e_3)\ E_{yo}\ A\theta_D}{K \qquad D}$$

Let

$$\chi = A^2 \phi_2 + C \ . \tag{6.22}$$

Hence equation (6.21) reduces to

$$\frac{\partial^4 \chi}{\partial z^4} + A^2 \chi = 0 \tag{6.23}$$

which is similar to equation (5.46) of the previous chapter. The general solution is of the form,

$$\begin{aligned} \chi \ = \ & C_1 \sin bz \sinh bz + C_2 \cos bz \cosh bz \\ & + C_3 \cos bz \sinh bz + C_4 \sin bz \cosh bz \end{aligned} \tag{6.24}$$

where $b = \sqrt{A/2}$ and C_1, C_2, C_3 and C_4 are coefficients to be determined from the boundary conditions. Hence

$$\phi_2(z) = \frac{1}{A^2}[C_1 \sin bz \sinh bz + C_2 \cos bz \cosh bz + C_3 \cos bz \sinh bz + C_4 \sin bz \cosh bz - C] . \quad (6.25)$$

Substituting for $\phi_2(z)$ in equation (6.20), we get

$$\phi_1(z) = \frac{1}{A^2}[C_1 \cos bz \cosh bz - C_2 \sin bz \sinh bz - C_3 \sin bz \cosh bz + C_4 \cos bz \sinh bz] . \quad (6.26)$$

We will consider three possible boundary conditions in these cells.

(a) Strong anchoring at both surfaces of the cell

At the lower plate, i.e., at $Z=0$, $\theta = 0$,

$$\phi_{1l}(o) = \phi_{2l}(o) = 0 .$$

Using these in equations (6.25) and *(6.26)* we get

$$C_1 = 0 \quad \text{and} \quad C_2 = C .$$

At the upper plate, i.e., at $Z = D$, $\theta = \theta_D$,

$$\phi_{1u}(D) = \phi_{2u}(D) = 0 .$$

Using these in equations *(6.25)* and *(6.26)* we get,

$$C_3 = \frac{C_4 \cos bD \sinh bD - C \sin bD \sinh bD}{\sin bD \cosh bD}$$

and

$$C_4 = \frac{C\{\frac{\sin bD \sinh bD \times \cos bD \sinh bD}{\sin bD \cosh bD} - \cos bD \cosh bD + 1)}{\{\frac{(\cos bD \sinh bD)^2}{\sin bD \cosh bD} + \sin bD \cosh bD\}}$$

(b) Assuming strong anchoring at the lower plate, and weak anchoring at tlie upper plate, we can calculate tlie coefficients as follows.

At the lower plate, i.e., at $Z=0$; $\theta=0$, $\phi_{1l}(o) = \phi_{2l}(o) = 0$.

From equations (6.25) and (6.26) we get as before, $C_1 = 0$ and $C_2 = C$.

At the upper plate, i.e., at $Z = \mathrm{D}, \mathrm{O} = \theta_D$, where there is weak anchoring, $\phi_{1u}(D)$ and $\phi_{2u}(D)$ are non-zero. Assuming the surface energy density to be of the form

$$F_s = \frac{1}{2} W_u \sin^2 \phi_D \,, \tag{6.27}$$

we can write the surface torque balance equation as follows:

$$\frac{W_u \sin 2\phi_D}{2} - K \cos^2 0 \left(\frac{\partial \phi}{\partial z}\right)_{\mathrm{D}} + \frac{E_y e_3 \sin 2\theta \cos \phi_D}{2} = 0 \,. \tag{6.28}$$

Let ϕ_{1u} and ϕ_{2u} be the amplitudes of the in-phase and out of phase components of ϕ at the upper plate. Linearising the equation (6.28), we can write, since $E_y = E_{yo} \sin \omega t$,

$$W_u \phi_{1u} - K \cos^2 \theta_D \left(\frac{\partial \phi_1}{\partial z}\right)_{\mathrm{D}} + \frac{E_{yo} e_3 \sin 2\theta_D}{2} = 0 \tag{6.29}$$

and

$$W_u \phi_{2u} - K \cos^2 \theta_D \left(\frac{\partial \phi_2}{\partial z}\right)_D = 0 \,. \tag{6.30}$$

Now using equations (6.25) and (6.26) in equations (6.29) and (6.30) the coefficients C_3 and C_4 can be calculated. (c) In general, we can have weak anchoring at both surfaces of the cell. In this case, the coefficients C_1, C_2, C_3 and C_4 can be calculated as follows.

At tlie lower plate, i.e., at $Z=0$, $\theta=0$. Let W_l be the anchoring energy and ϕ_{1l} arid ϕ_{2l} the amplitudes of the in-phase and out of phase components of ϕ at this plate. Then linearising tlie surface torque balance equation of the form of equation (6.28) with respect to ϕ_{1l} and ϕ_{2l} we get,

$$\frac{\partial \phi_{1l}}{\partial z} = \left(\frac{W_l}{K}\right) \phi_{1L} \quad \text{and} \quad \frac{\partial \phi_{2l}}{\partial z} = \left(\frac{W_l}{K}\right) \phi_{2l} \,. \tag{6.31}$$

At the upper plate, i.e., at $Z = \mathrm{D}$, $\theta = \theta_D$, we write the torque balance equations (6.29) and (6.30) as described in the previous section (b).

Now using the equations (6.25), (6.26), (6.29), (6.30) arid (6.31), we can calculate the coefficients C_1, C_2, C_3, and C_4. The calculation is straightforward but tedious. We will not give tlie explicit expressions for C_1 to C_4.

6.5 Calculation of Intensity of Transmitted Light

From equation (6.2) with $\psi = 22.5°$, the transmitted intensity is given by

$$T_i = \frac{(1 - \cos \Delta\Phi)}{4} \tag{6.32}$$

where the phase difference,

$$\Delta\Phi = \frac{2\pi}{\lambda}\Delta l \tag{6.33}$$

arid Al, tlie path difference of tlie cell is given by

$$\Delta l = \int_o^d [n_{eff}(z) - n_o]dz \tag{6.34}$$

where

$$n_{eff} = \frac{n_o}{\sqrt{1 - \mathrm{R}\sin^2\theta}} \quad \text{and} \quad \mathrm{R} = \frac{n_e^2 - n_o^2}{n_e^2} \tag{6.35}$$

n_e and n_o arc refractive indices of tlie medium for extraordiriary and ordinary rays.

Since both θ and ϕ vary with Z in the nematic cell, the calculation of intensity should take into account both variations. For the purpose of calculatiori of optical transmission through the medium, we cut the sample into a number of slices of equal thickness Ad along tlie Z axis. Then we calculate the phase acquired by tlie light beam passing through the slice, which depends on the local tilt angle θ. We assume each slice makes a uniform azimuthal angle ϕ, which is equal to that at the centre

of the slice and a uniform tilt angle θ, which again corresponds to that at the centre of the cell.

Let ϕ_o be the angle between the polariser and $\vec{m}_1$, which is the projection of $\hat{n}$ at the centre of the first slice on the surface of the cell. Let E_o be the amplitude of the electric vector of tlie incident light beam at any given instant (Fig.6.11). Then the component of E_o along $\vec{m}_1$ is $E_{\|}^{in}(1) = E_o \cos\phi_o$ and the component of E_o perpendicular to $\vec{m}_1$ is given by $E_{\perp}^{in}(1) = E_o \sin\phi_o$. Then the component of the field parallel to $\vec{m}_1$ after the light beam emerges from the first slice are (Fig.6.11) $E_{\|}^{o}(1) = E_{\|}^{in}(1)\, e^{i\alpha_1}$.

Mere α_1 is the phase angle acquired by the light beam and is given by

$$\alpha_1 = \frac{2\pi}{\lambda} n_{eff}\, \Delta d$$

where, n_{eff} is given by equation (6.35).

Similarly the component orthogonal to $\vec{m}_1$ is given by $E_{\perp}^{o}(1) = E_{\perp}^{in}(1)\, e^{i\alpha_o}$ where $\mathrm{a}, = \frac{2\pi}{\lambda} n_o \Delta d$. The components of the electric field of the light beam incident on the next slice are given by,

$$E_{\|}^{in}(2) = E_{\|}^{o}(1)\cos\Delta\phi_{12} + E_{\perp}^{o}(1)\sin\Delta\phi_{12}$$

$$\text{and} \quad E_{\perp}^{in}(2) = E_{\perp}^{o}(1)\cos\Delta\phi_{12} - E_{\|}^{o}(1)\sin\Delta\phi_{12}$$

where $\Delta\phi_{12}$ is tlie angle made by tlie projection of tlie director at tlie centre of tlie second slice on the XY plane, i.e., $\vec{m}_2$ with $\vec{m}_1$ (Fig.6.11).

After passing through the second slice the electric field components are given by

$$E_{\|}^{o}(2) = E_{\|}^{in}(2)e^{i\alpha_2} \text{ and } E_{\perp}^{o}(2) = E_{\perp}^{in}(2)e^{i\alpha_o}.$$

Continuing the calculations in the same way the light beam coming from the last, i.e., N^{th} slice has tlie components of the field given by

$$E_{\|}^{o}(N) = E_{\|}^{in}(N-1)\, e^{i\alpha_N} \text{ parallel to } \vec{m}_N \text{ and}$$

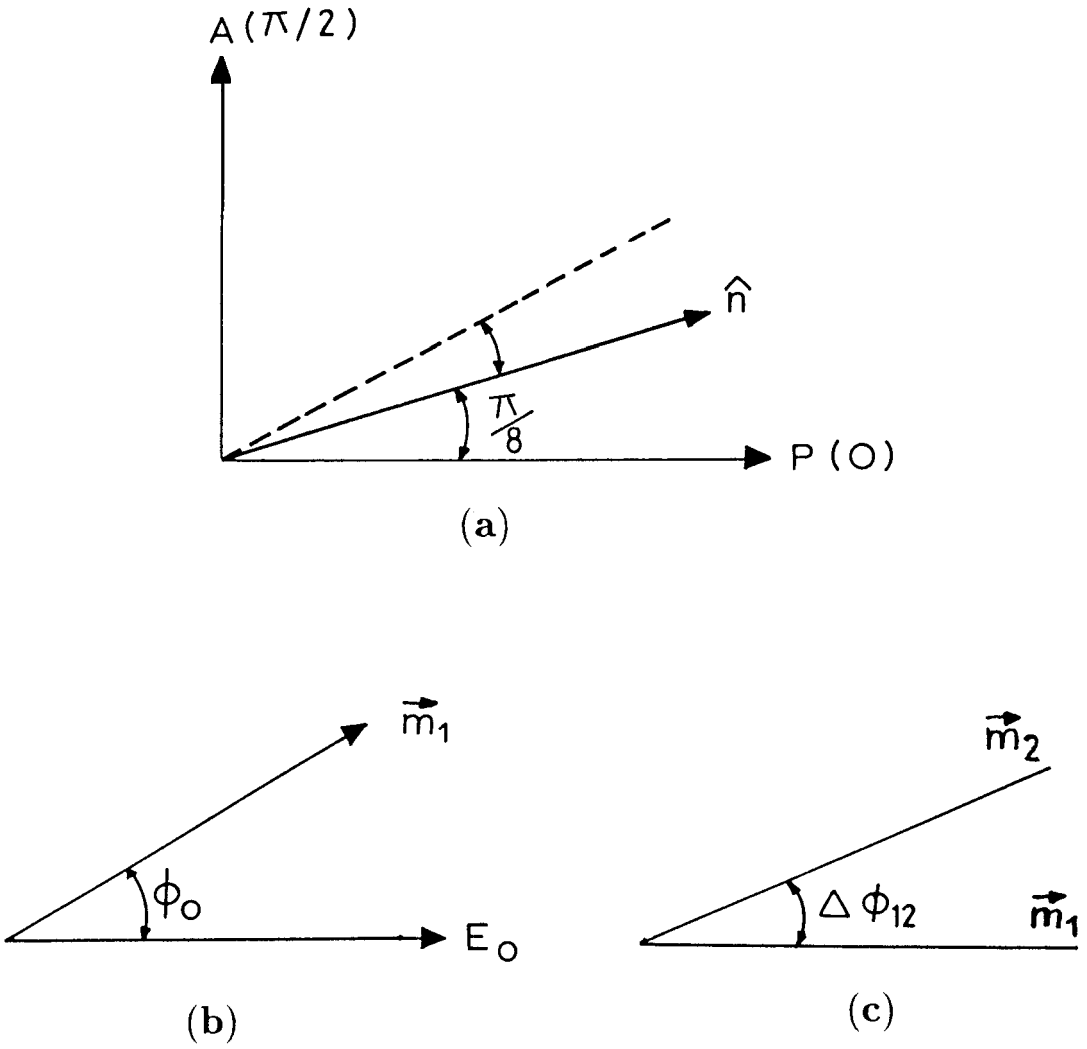

Fig.6.11 (a) P is the polarizer, A is the analyser, $\hat{n}$ is the nematic director at tlie lower plate and tlie dotted line represents the projection of $\hat{n}$ at the upper plate; (b) m_1 is the projection of tlie director in the centre of the first slice on the XY plane. E_o is the amplitude of the electric vector of the incident light beam. (c) $\vec{m}_1$ and $\vec{m}_2$ are the projections of the director at the centres of first and second slices respectively on the XY plane.

$$E^o_{\perp}(N) \;=\; E^{in}_{\perp}(N-1)\, e^{i\alpha_o} \text{ perpendicular to } \vec{m}_N.$$

Therefore the resultant electric field of the emergent light beam is given by,

$$E^o = E^o_{\parallel}(N)\cos\phi_1 + E^o_{\perp}(N)\sin\phi_1$$

where ϕ_1 is the azimuthal angle between the analyser (which is crossed with respect to the polariser) and $\vec{m}_N$.

The intensity of the emergent light is given by $I^o = E^o E^{o*} = \mid E^o \mid^2$, where E^{o*} is the complex conjugate of E^o. The in-phase and out of phase components of the transmitted intensities are given by

$$I_1 = \mid E^o(1) \mid^2 \quad \text{and} \quad I_2 = \mid E^o(2) \mid^2$$

where $E^o(1)$ and $E^o(2)$ are the electric fields of the emergent light corresponding to $\phi_1(z)$ and $\phi_2(z)$ profiles respectively.

Therefore the time-dependent parts of the in-phase and out of phase components of the intensity of transmitted light can be written as

$$D_1 = I_1 - I_0 \quad \text{and} \quad D_2 = I_2 - I_0$$

where I_o is the time-independent DC part which can be calculated using equation (6.33). Hence the net intensity of the f component of the transmitted light is given by $\mathbf{I} = \sqrt{D_1^2 + D_2^2}$ and the phase of the output light beam in relation to the applied AC electric field is given by $\delta_I = tan^{-1}[D_2/D_1]$.

In the above calculations θ, $\phi_1(z)$ and $\phi_2(z)$ are calculated using equations (6.16), (6.26) and (6.25) respectively.

6.6 Discussion

Using cells made of glass plates both of which are treated with SiO for zero pretilt angle, the electrooptical signal at the frequency of the applied field is not observed.

This indicates that the azimuthal anchoring energy is strong for SiO coating, which gives rise to zero pretilt angle.

We have calculated the transmitted intensity as a function of pretilt angle at tlie top surface by assuming fixed boundary conditions at the two surfaces (Fig.6.12). These calculations are made for a typical cell of thickness (D) = 23 μm, at an applied AC electric field of $0.083 \times 10^5 V/m$ and at a frequency of 20 Hz.

The material parameters used in the calculations at 313 K are:

K = 5.67 x 10^{-12} N (Schad et al., 1981);

$n_e = 1.5814$ and $n_o = 1.4825$ (Sen *et al.*, 1985);

$\gamma_1 = 0.03$ $\mathrm{Kgm^{-1}s^{-1}}$; $e_1 - e_3 = 6.7$ x 10^{-12} C/m.

The value of γ_1 used in the calculations is more than the value given in tlie Merck manual. Further the value of $(e_1 - e_3)$ used in the calculations is lower than our own experimentally measured value of $8.8 \times 10^{-12} Cm^{-1}$. These changes in γ_1 and $(e_1 - e_3)$ are made in order to get a better agreement of the calculated values with the experimental data, as will be discussed later. It is convenient to show the results by taking the ratio of f signal to DC signal per unit field E. From figure 6.12 it is clear that the curve passes through the origin, i.e., when the pretilt angle θ_D is zero, the transmitted intensity is also zero as we have found in the experiment. The f signal increases with the increase in the pretilt angle as can be expected. In figure 6.13 we illustrate the vriations of the in-phase (ϕ_1) and the out of phase (ϕ_2) amplitudes of ϕ across the cell thickness D. ϕ_2 has larger amplitude than ϕ_1, which indicates a large dissipative loss in the medium.

We have conducted experiments on a cell with one plate coated with SiO to get a large pretilt angle (20°) and the other to get zero pretilt angle. In such a cell there is a splay-bend deformation of the director orientation, which gives rise to ϕ

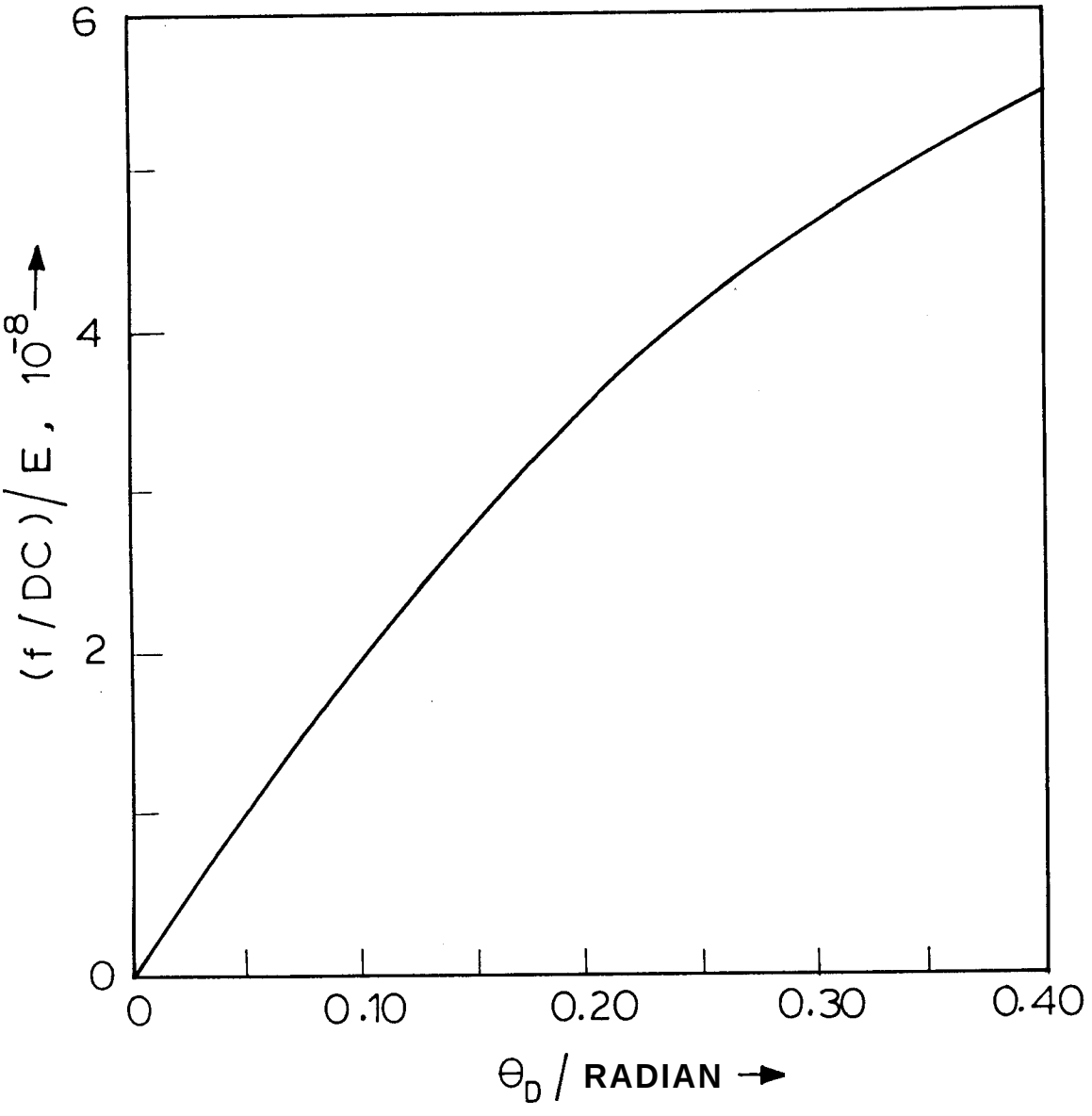

Fig.6.12 Calculated transmitted intensity per unit field E, $\left[\left(\frac{f\ signal}{\mathrm{DC}\ signal}\right)/E\right]$ as a function of pretilt angle at the top surface assuming fixed boundary conditions.

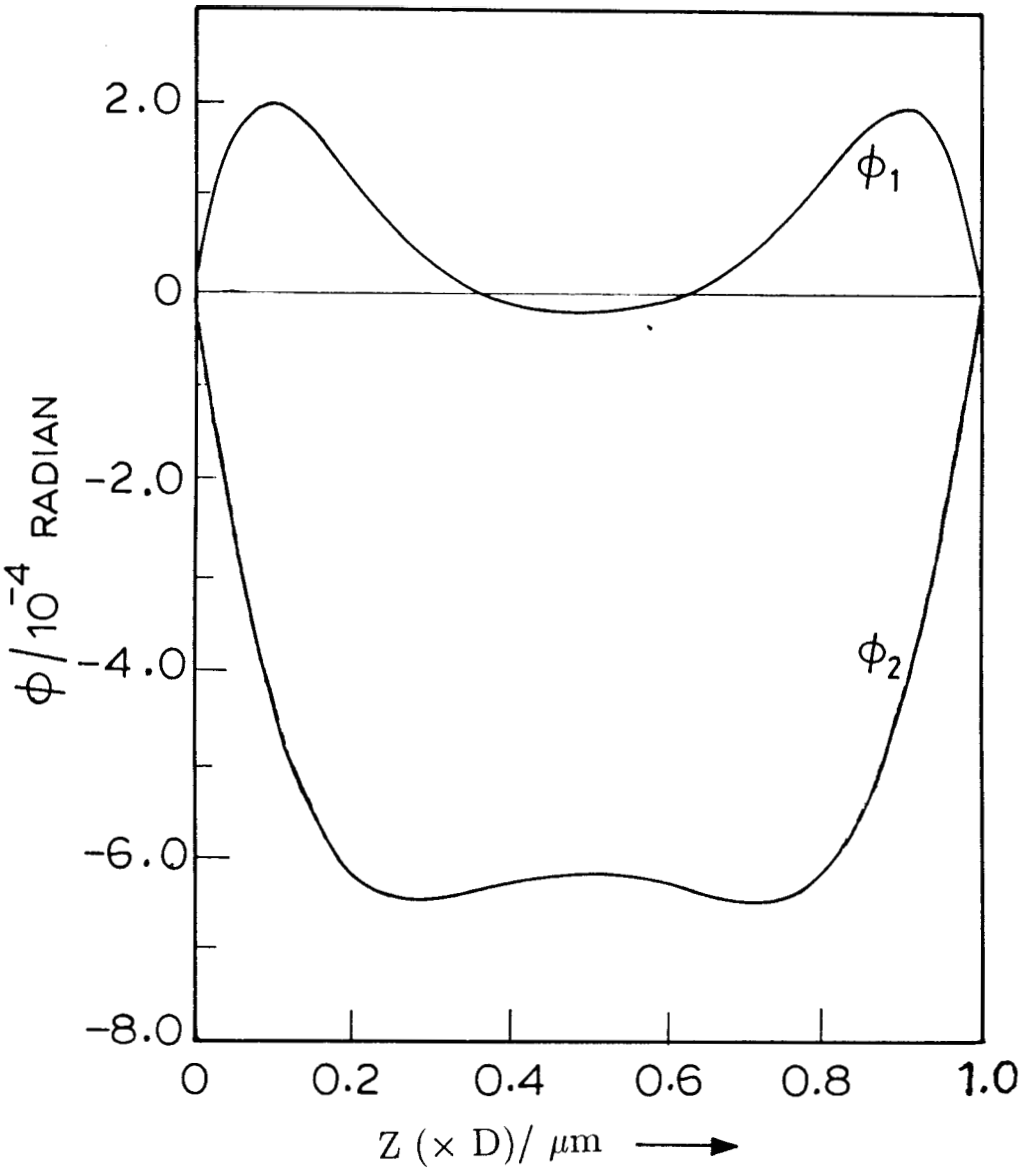

Fig.6.13: Calculated in-phase (ϕ_1) and out of phase (ϕ_2) oscillations across the cell thickness D = 24.2 μm assuming strong anchoring at the boundaries.

oscillations and hence to a f signal at the frequency of the applied field. Calculations made on the assumption that the anchoring is strong at the two surfaces of the cell broadly agree with the experimental values.

Figures 6.14 and 6.15 show calculated values of transmitted intensity as a function of field and frequency of the field respectively. These calculations are made for the cell thickness D=24.2 μm and the pretilt angle $\theta_D = 0.35$ radians.

There is a broad agreement between the calculated values (Fig. 6.15) and experimental numbers in the frequency range of 20 Hz to 40 Hz as shown in Table 6.1 when $(e_1 - e_3)$=$6.7\times10^{-12}C/m^{-1}$. We may note that the value of γ_1 of PCH-7 quoted in the Merck manual is 0.03 $Kgm^{-1}s^{-1}$ at a temperature of 293 K. Hence γ_1 can be expected to be even lower at 313 K. However, in order to get a better agreement between the calculated values and the experimental data for the frequency dependence, we had to use $\gamma_1 \simeq 0.03$ $Kgm^{-1}s^{-1}$ at 313 K.

In figure 6.15 we have also shown the frequency response of transmitted intensity, calculated for $(e_1 - e_3)$=$6.7\times10^{-12}Cm^{-1}$. Using our measured value of $(e_1 - e_3)$, i.e., $8.8\times10^{-12}Cm^{-1}$ (as described in Chapter IV), the calculated transmitted intensity is higher than the experimental data at all the frequencies (see Table 6.2). Hence we have reduced $(e_1 - e_3)$ to $6.7\times10^{-12}Cm^{-1}$ to get a better agreement with the experimental values. Therefore if other parameters are known and if there is strong anchoring at the two boundaries, this sensitive dependence of the transmitted intensity can be used to measure $(e_1 - e_3)$ of nematic liquid crystals.

As explained in the experimental section, we have also done measurements using cells with the upper plate coated with polyimide and the lower plate coated with SiO to get zero pretilt angle. The signal from such a cell is much smaller than the previous case with a large pretilt angle at the upper surface. Assuming strong

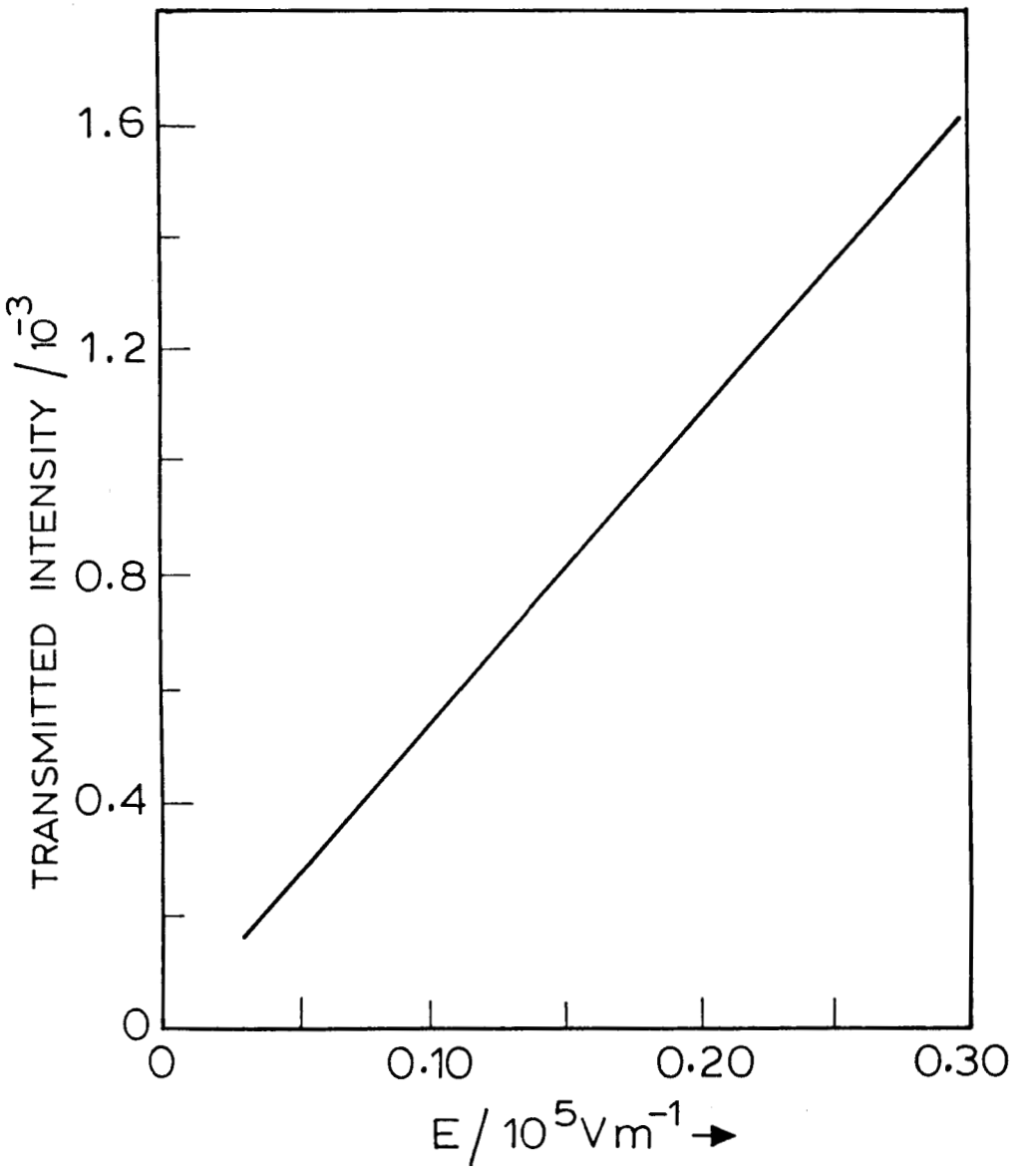

Fig.6.14: Calculated transmitted intensity (f signal/DC signal) as a function of the electric field assuming fixed boundary conditions.
D=24.2 μm, θ_D=0.35 radians.

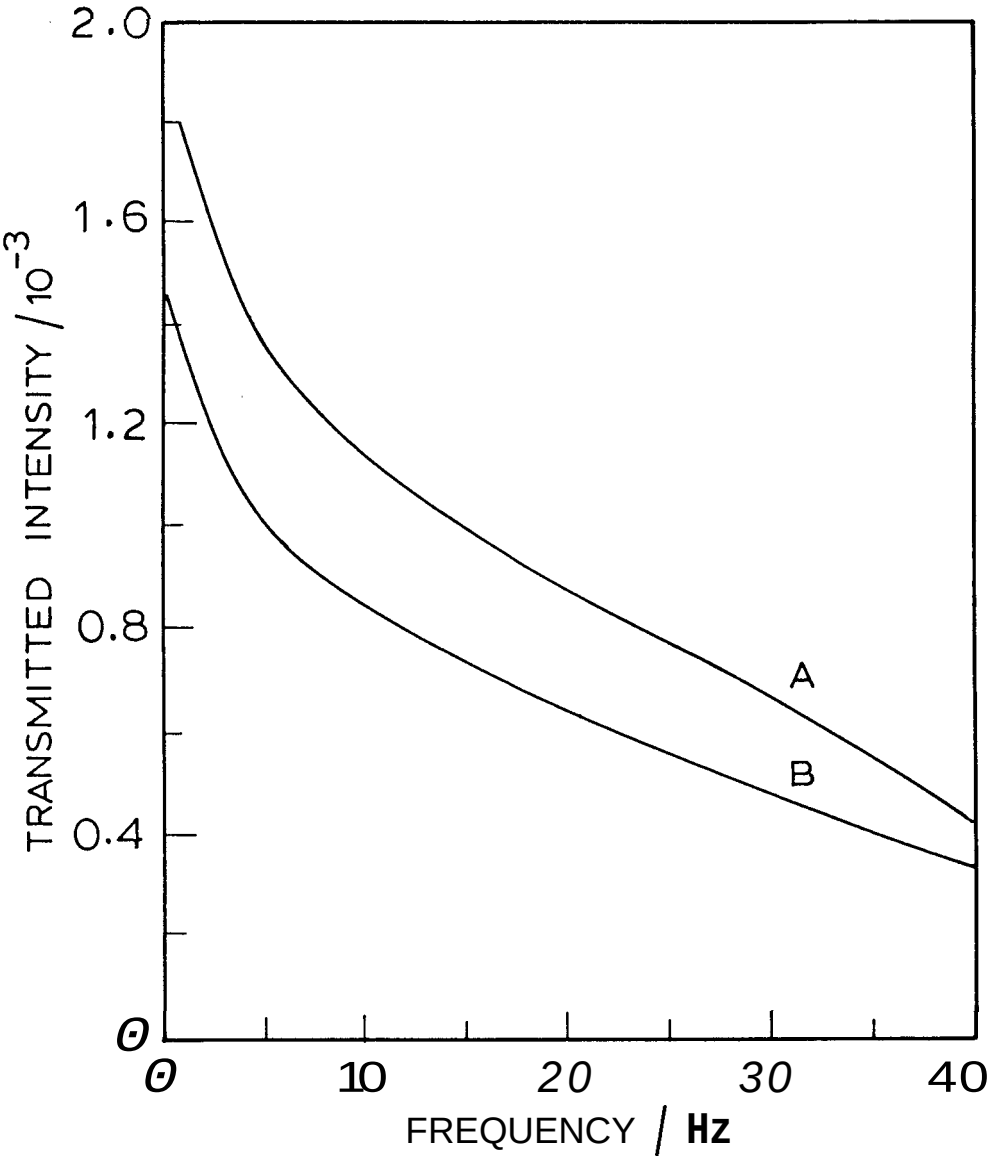

Fig.6.15: Transmitted intensity (f signal/DC signal) as a function of frequency for A: $(e_1 - e_3) = 8.8 \times 10^{-12} C/m$ and B: $(e_1 - e_3)=6.7 \times 10^{-12} C/m$ (fixed boundary conditions). $D=24.2\ \mu m$, $E_o=0.083\times10^5 V/m$.

Table 6.1

Comparison of calculated and experimental values of the transmitted signal for a cell with its top plate coated with SiO to get large pretilt angle.

Frequency of the AC field	Value of $[f\ signal/DC\ signal]/E_o$	
	Experimental (Fig.6.7)	Calculated (Fig.6.15)
20 Hz	7.9 e-8	8.0 e-8
30 Hz	6.0 e-8	6.1 e-8
40 Hz	5.4 e-8	5.4 e-8

Table 6.2

Comparison of calculated and experimental data of transmitted intensity at different values of $(e_1 - e_3)$ for **a** cell with its top plate coated with SiO to get large pretilt angle.

Frequency	Caculated value of transmitted intensity (fig.G.15)		Experimental (Fig.6.7)
	e_1-e_3=8.8×10^{-12}Cm^{-1}	e_1-e_3=6.7×10^{-12}Cm^{-1}	
20 Hz	0.88 x	0.64 x	0.70 x
30 **Hz**	0.73×10^{-3}	0.54×10^{-3}	0.52×10^{-3}
40 Hz	0.48×10^{-3}	0.35×10^{-3}	0.35×10^{-3}

anchoring at both the surfaces, we get a slope of the transmitted intensity vs. field as $\approx 0.9\times10^{-8}m$ assuming the material parameters as given in the beginning of this section at a temperature of 313 K and D=22.8 μm. The pretitlt angle is assumed to be θ_D=0.034 as measured by the crystal rotation method (see section 2.5.2 of Chapter II). This value of the slope is smaller than the experimental value of $6.7\times10^{-8}m$ measured at 313 K for a cell of the same thickness. As we have already found in this section, SiO coating gives rise to a strong anchoring. We have also made calculations by assuming the polyimide coating gives rise to a relatively weak anchoring using equations (6.29) and (6.30). Using W_u=$2.7\times10^{-6} J/m^2$ for the polyimide coated plate the slope of the transmitted intensity vs. field is $\approx 6.5\times10^{-8}m$ (Fig.6.16). This is comparable with the experimental data (Table 6.3).

Figure 6.17 shows the calculated variations in the in-phase and out of phase components of $\phi(z)$ across the cell thickness for the parameters mentioned above. ϕ_1 and ϕ_2 vary strongly near the weakly anchored upper surface. Comparing the ϕ profile when the upper surface is also characterised by strong anchoring (Fig.6.13) in the weakly anchored case the ϕ profile is assymmetric.

We have also made calculations of the transrnitted intensity as a function W_u. The results are shown in figure 6.18. As the anchoring energy W_u increases, the transrnitted intensity also increases and curiously reaches a maximum value and then again decreases. On the other hand, the phase (line AB) reverses sign after reaching $\pi/2$ radians before the transmitted intensity reaches a maximum. At higher value of W„ the phase angle decreases continuously. We have also plotted in figures 6.19a-d the Z-dependences of the in-phase (ϕ_1) and the out of phase (ϕ_2) components of ϕ for different values of W_u, viz., $1\times10^{-6} J/m^2$, $2.2\times10^{-6} J/m^2$, $3.0\times10^{-6} J/m^2$ and $4.4\times10^{-6} J/m^2$ rcspcctivcly and D=22.8 μm, θ_D=0.034 radians. The output

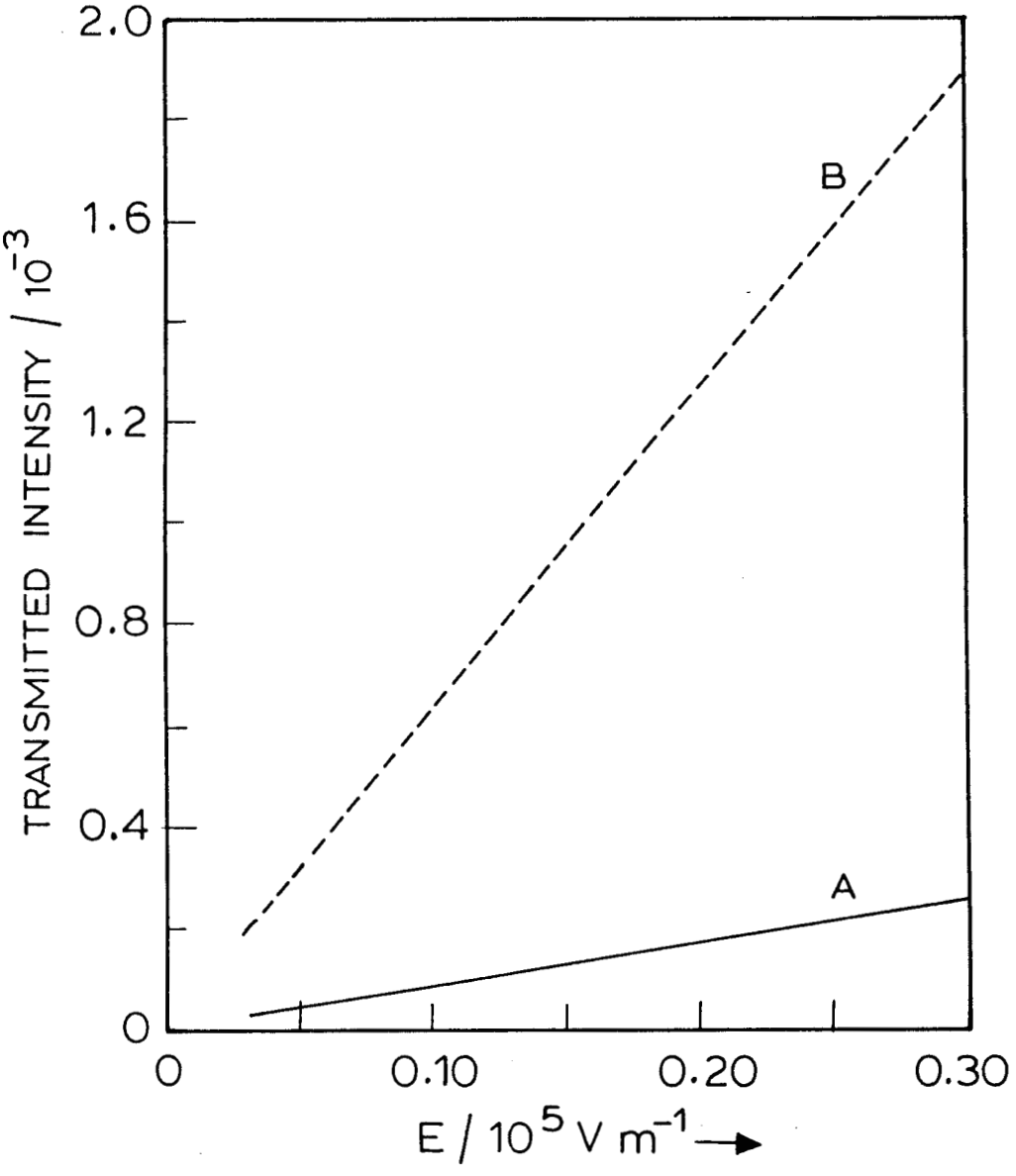

Fig.6.16: Calculated transmitted intensity (f signal/DC signal) as a function of the electric field assuming strong anchoring at both the plates of the cell (line A) and assuming $W_u = 2.7\times10^{-6} Jm^{-2}$ and strong anchoring at the lower plate (Line B). Cell thickness (D) = *22.8* μm and a pretilt angle $\theta_D = 0.034$ radians at the upper plate.

Table 6.3

Values of $\left(\frac{f\ signal}{DC\ signal}\right)/E$ at 7 Hz. D = 22.8 μm, $\theta_D = 0.034$ radians, inter-electrode spacing = 1250 μm for a cell with its top plate coated with polyimide.

Experimental value (Fig.6.9)	6.7 x $10^{-8} m$
Calculated value assuming strong anchoring at both the plates (Fig.6.16 Curve A)	0.9 x $10^{-8} m$
Calculated value assuming weak anchoring at the upper plate. W_u = 2.7 x 10^{-6} Jm^{-2} (Fjg.6.16 Curve B)	6.5 x $10^{-8} m$

The physical parameters used in these calculations are given in Section 6.6.

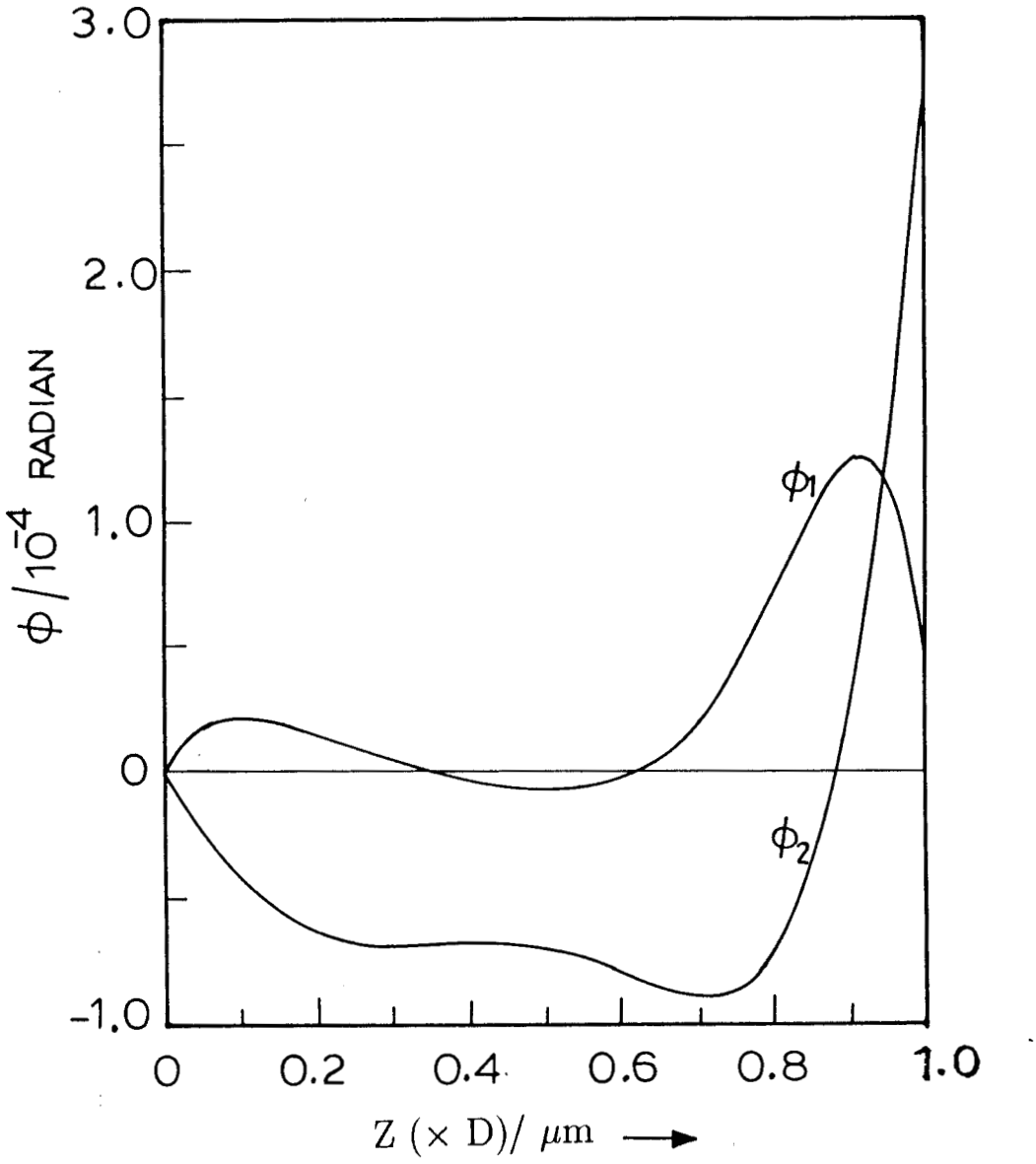

Fig.6.17: Profiles of in-phase (ϕ_1) and out of phase (ϕ_2) components of the azimuthal angle of the director across the cell thickness, D=22.8 μm, W_u=2.7 x $10^{-6} Jm^{-2}$ and θ_D = 0.034 radians, E_o=0.083×$10^5 V/m$, frequency = 7 Hz.

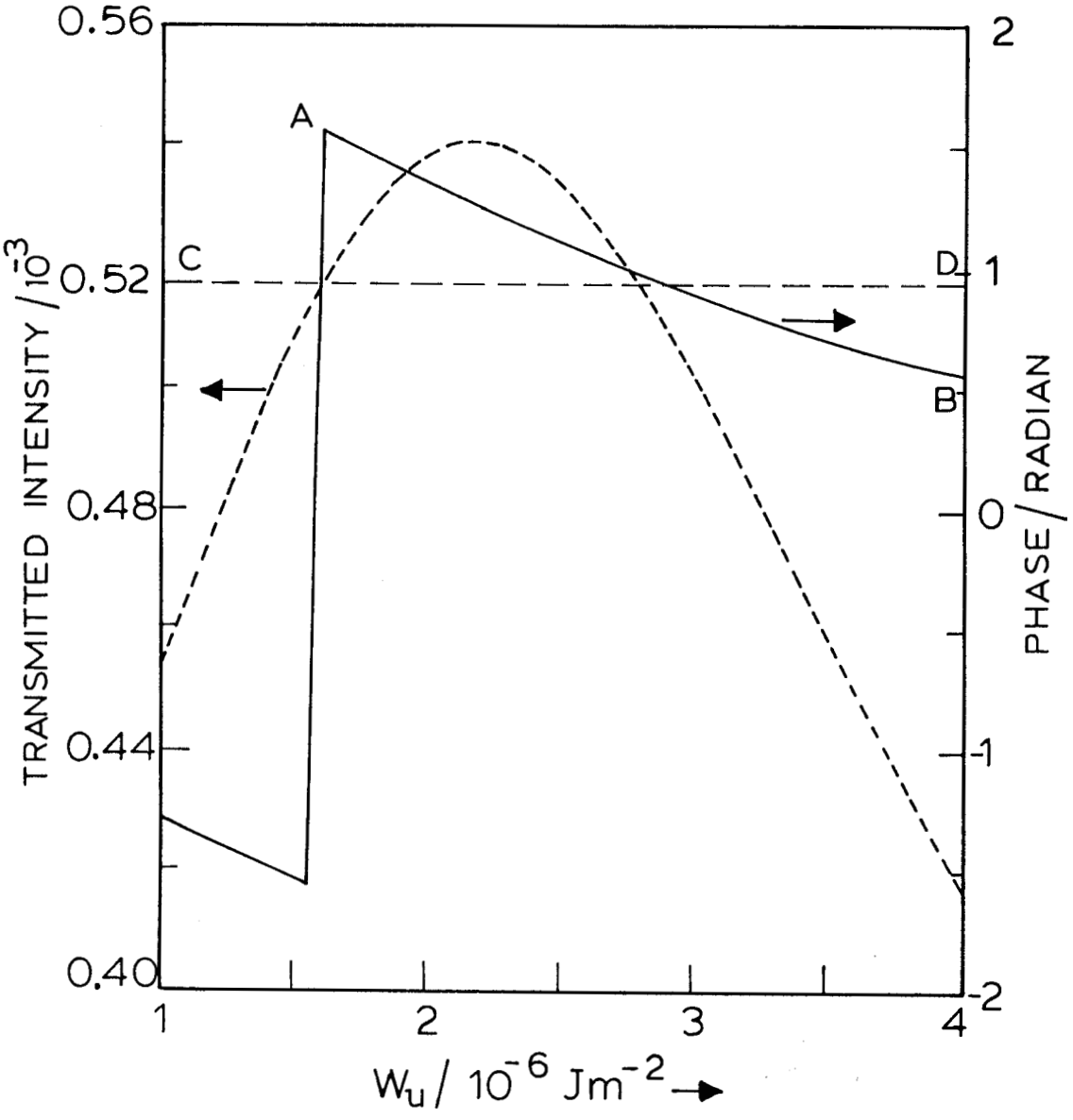

Fig.6.18: Transmitted intensity (f signal/DC signal) and phase (δ) as a function of anchoring energy, W_u at the upper plate. The line CD has been drawn to show the experimental value of phase angle. $D = 22.8\mu m$, $\theta_D = 0.034$ radians.

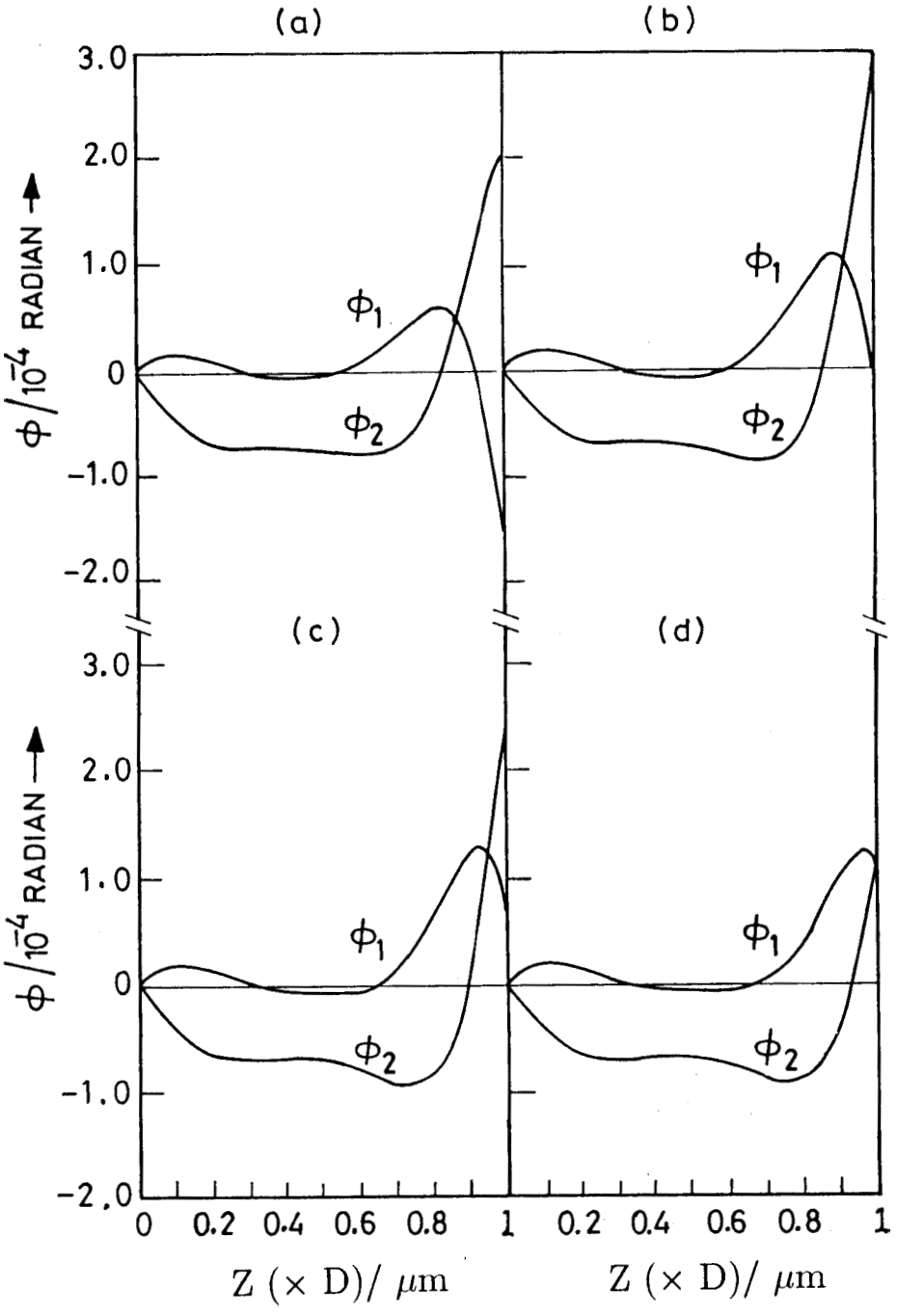

Fig.6.19: Calculated in phase (ϕ_1) and out of phase (ϕ_2) components of the azimuthal angle of the director across cell thickness, D = 22.8 μm; $\theta_D = 0.034$ radians; (a) $W_u = 1 \times 10^{-6} Jm^{-2}$, $(b) W_u = 2.2 \times 10^{-6} Jm^{-2}$, (c) $W_u = 3.0 \times 10^{-6} Jm^{-2}$ and (d) $W_u = 4.4 \times 10^{-6} Jm^{-2}$.

intensity can be expected to depend sensitively on an appropriate average value of ϕ_1 and ϕ_2 at the top surface. From these figures it is clear that ϕ_1 and ϕ_2 are themselves very sensitive to variations of W_u. At the upper surface the in-phase component ϕ_1 has a large negative value for a low value of W_u (= 1 x $10^{-6}\,J/m^2$). But as the value of W_u increases the negative value of ϕ_1 decreases and after passing through zero becomes positive and increases again. However ϕ_2 is always positive and as W_u increases ϕ_2 reaches a maximum value at $W_u = 2.2\times10^{-6}\,J/m^2$ before decreasing again with W_u. The observed maximum in the amplitude of f signal is connected with this sensitive dependence of the ϕ_1 and ϕ_2 profiles on W_u. From figure 6.18 it is clear that for a given value of transmitted intensity, there are two possible values of W_u. However, the phase of the optical signal at the two values of W_u are quite different. In our experiment (Fig.6.9) the relative value of the transmitted intensity (f signal/DC signal) is 5×10^{-4}. Taking into account the phase inversion by the preamplifier, the experimental value of the phase angle is 0.91 radians. Comparing these experimental values of intensity and phase with the calculated values, we estimate from figure 6.18 that $W_u \simeq 2.7\times10^{-6}\,J/m^2$.

Faetti and Lazzari (1992) have measured W_ϕ for 5CB. They used glass plates treated with SiO vapour to get zero pretilt angle of the nematic director at the surface. Their value of W_ϕ is of the order of $10^{-5}\,J/m^2$ at the nematic-isotropic transition temperature. This value implies a fairly strong anchoring at the SiO coated glass plate. our first experiment using SiO coated glass plates shows that PCH-7 also has a strong anchoring on this surface. On the other hand, our measurements of W_ϕ for PCH-7 aligned on polyimide coated glass plate gives a lower value of the anchoring energy.

References

BARBERO,G., MIRALDI,E., OLDANO,C., RASTELLO,M.L. and TAVERNA VALABREGA, P, 1986, *J.* de Phys., 47, 1411.

BODENSCHATZ,E., ZIMMERMANN,W. and KRAMER,L., 1988, **J.** de Phys., 49, 1875.

DE GENNES,P.G., 1975, The Physics of Liquid Crystals (Clarendon Press,Oxford).

DURAND,G., 1993, Liquid Crystals, 14, 159.

FAETTI,S., GATTI,M. and PALLESCHI,V., 1986, Rev. Phys. Appl., 21, 451.

FAETTI,S. and PALLESCHI,V., 1987, Liquid Crystals, 2, 261.

FAETTI,S. and LAZZARI,C., 1992, **J.** Appl. Phys., 71, 3204.

GUYON,E., PIERANSKI,P. and BOIX,M., 1973, Lett. Appl. Eng. Sci., I 19.

JANNINGS,J.L., 1972, Appl. Phys. Lett., **21**, 173.

MONKADE,M., BOI,M. and DURAND,G., 1988, *Europhys.* Lett., 5, 697.

MOSLEY,A., NICHOLAS, B.M. and GASS,P.A., 1987, Displays, **8,** 17.

SCHAD,Hp. and OSMAN,M.A., 1981, **J.** Chem. Phys., 75, 880.

SEN,S.,KALI,K.,ROY,S.K.and ROY,S.B., 1985, Mol.*Cryst.*Liquid *Cryst.*,**126**, 269.

SICART,J., 1976, **J.** de Phys. Lett., 37, L-25.

TOSHIO OH-IDE, SEIYU KUNIYASU and SHUNSUKE KOBAYASHI, 1988, Mol. *Cryst.* Liquid *Cryst.*, 164, 91.

ERRATA

1) In page 45, line 14 should read: "... is expected to increase with increase in temperature."

2) Figure 4.10 is to be modified as follows:

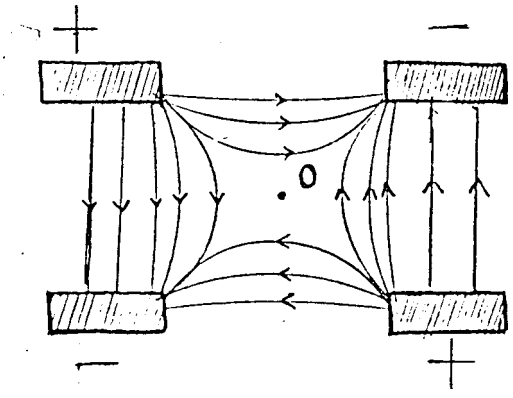

Fig.4.10: Schematic diagram showing formation of field gradient in a quadrupolar cell.